Green Chemistry

PAPER

View Article Online
View Journal | View Issue

Cite this: *Green Chem.*, 2019, **21**, 5852

Niobium oxide prepared through a novel supercritical-CO_2-assisted method as a highly active heterogeneous catalyst for the synthesis of azoxybenzene from aniline†

Yehan Tao, Bhawan Singh, Vanshika Jindal, Zhenchen Tang and Paolo P. Pescarmona *

High-surface area Nb_2O_5 nanoparticles were synthesised by a novel supercritical-CO_2-assisted method (Nb_2O_5-$scCO_2$) and were applied for the first time as a heterogeneous catalyst in the oxidative coupling of aniline to azoxybenzene using the environmentally friendly H_2O_2 as the oxidant. The application of $scCO_2$ in the synthesis of Nb_2O_5-$scCO_2$ catalyst resulted in a significantly enhanced catalytic activity compared to a reference catalyst prepared without $scCO_2$ (Nb_2O_5-Ref) or to commercial Nb_2O_5. Importantly, the Nb_2O_5-$scCO_2$ catalyst achieved an aniline conversion of 86% (stoichiometric maximum of 93% with the employed aniline-to-H_2O_2 ratio of 1 : 1.4) with an azoxybenzene selectivity of 92% and with 95% efficiency in H_2O_2 utilisation in 45 min without requiring external heating (the reaction is exothermic) and with an extremely low catalyst loading (weight ratio between the catalyst and substrate, $R_{c/s}$ = 0.005). This performance largely surpasses that of any other heterogeneous catalyst previously reported for this reaction. Additionally, the Nb_2O_5 catalyst displayed high activity also for substituted anilines (*e.g.* methyl or ethyl-anilines and *para*-anisidine) and was reused in consecutive runs without any loss of activity. Characterisation by means of N_2-physisorption, XRD, FTIR and TEM allowed the correlation of the remarkable catalytic performance of Nb_2O_5-$scCO_2$ to its higher surface area and discrete nanoparticle morphology compared to the aggregated larger particles constituting the material prepared without $scCO_2$. A catalytic test in the presence of a radical scavenger proved that the reaction follows a radical pathway.

Received 26th July 2019,
Accepted 11th September 2019

DOI: 10.1039/c9gc02623a

rsc.li/greenchem

Introduction

Over the past few years, azoxybenzene and its derivatives have garnered interest due to their importance in organic synthesis as intermediates for producing dyes or medicines, as inhibitors or stabilisers for polymerisation, and as liquid crystals in electronic displays.[1–4] For example, azoxybenzene is the precursor to prepare hydroxyazobenzene, a common azo dye, by Wallach rearrangement.[5] Reductive cleavage of azoxybenzene or its derivatives gives indazole derivatives, which have pharmaceutical activity.[6] Methoxy-substituted azoxybenzene, *i.e.* azoxyanisole, is one of the first known and most readily prepared liquid crystals.[7] In addition, exploration of the functionalisation of azoxybenzene, such as acylation or alkenylation, has also been reported.[8] Azoxybenzene can be synthesised either by oxidative coupling of aniline or by selective reduction of nitrobenzene or nitrosobenzene. The reduction route has been extensively studied, employing for example Ni–C–CeO_2,[9] Au–hydrotalcite,[10] Ag–Cu–ZrO_2,[11] and Pd–CdS[12] as catalysts. On the industrial scale, nitrobenzene is prepared by nitration of benzene with a mixture of concentrated sulphuric acid, nitric acid and water, whereas nitrosobenzene is prepared by reduction of nitrobenzene. Both of them are obtained from petroleum-based raw materials. On the other hand, the production of aniline from renewable resources (unrefined raw sugar) has been recently reported by Covestro,[13] which makes the oxidation route preferable from a green chemistry point of view.

Chemical Engineering Group, Engineering and Technology Institute Groningen (ENTEG), Faculty of Science and Engineering, University of Groningen, Nijenborgh 4, 9747 AG Groningen, The Netherlands. E-mail: p.p.pescarmona@rug.nl

†Electronic supplementary information (ESI) available: Image of the high-throughput $scCO_2$ reactor. Kinetic study of 20 mmol aniline conversion over the Nb_2O_5-$scCO_2$ catalyst. Pictures of 50 mmol aniline conversion over Nb_2O_5-$scCO_2$ and Nb_2O_5-Ref catalysts as a function of time. XRD pattern of Nb_2O_5-800°C. TEM pictures of Nb_2O_5-$scCO_2$. SEM images of Nb_2O_5-$scCO_2$ and Nb_2O_5-Ref catalysts. Pictures of conversion of aniline with different concentrations of H_2O_2 after 25 min. Plots of aniline conversion and products yields in different solvents. Reusability test of the Nb_2O_5-$scCO_2$ catalyst. Comparison with the previously reported heterogeneous catalysts. List of chemicals and their purity used in this work. Reaction pathway from the oxidative coupling of aniline with H_2O_2 to azoxybenzene over the Nb_2O_5-$scCO_2$ catalyst. See DOI: 10.1039/c9gc02623a

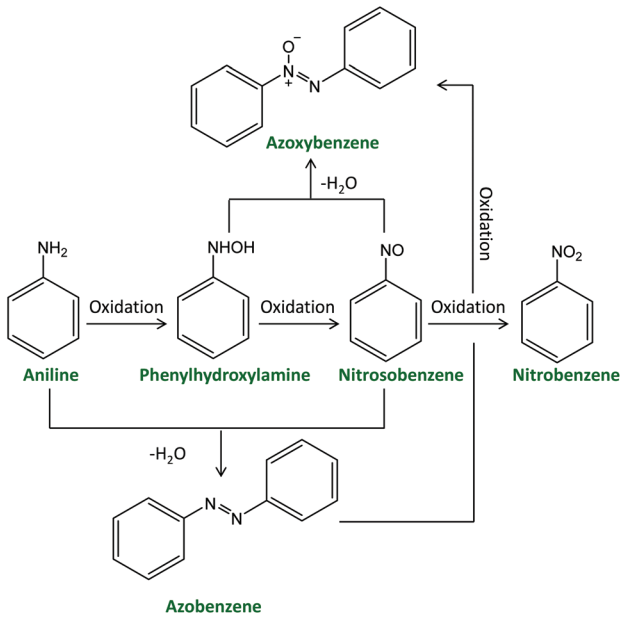

Scheme 1 Generally-accepted reaction scheme for the synthesis of azoxybenzene *via* the oxidation of aniline.

The oxidation route comprises competitive oxidation and condensation reactions (Scheme 1). Therefore, the reaction can generate several products, including phenylhydroxylamine,[14] nitrosobenzene,[15] azobenzene,[16] azoxybenzene[17] and nitrobenzene.[18] This represents a major challenge for achieving high selectivity towards a specific product, such as azo or azoxybenzene. Several metal-based heterogeneous catalysts have been applied in the oxidation of aniline and its substituted derivatives with the aim of selectively yielding azoxy products using H_2O_2 as the oxidant. H_2O_2 is an environmentally friendly oxidant as it gives water as the only side product, it can be operated at ambient pressure and more safely compared to molecular oxygen,[15,19] and is significantly cheaper and greener compared to other oxidants that have been reported for this reaction, such as peracetic acid,[20] *tert*-butylhydroperoxide, dimethyldioxirane,[21] sodium perborate *etc.*[22] An overview of the state-of-the-art heterogeneous catalysts for the oxidative coupling of aniline with H_2O_2 as the oxidant is shown in Table S1.† Ti-Based materials such as TiO_2[23–25] and Ti-silicates (TS-1,[26,27] Ti-MCM-48,[28] TAPSO-5, Ti-HMS, and Ti-Beta[29]) are the most common types of heterogeneous catalysts that have been reported for this reaction. They have been reported to activate H_2O_2 by forming hydroperoxo species.[23,28] Most of these Ti-based catalysts typically operate in the 50–70 °C temperature range, while the TiO_2 pillared montmorillonite clays (~60 wt% TiO_2) allowed the oxidation of aniline at room temperature (RT), reaching 50% aniline conversion with 99% azoxybenzene selectivity after 8 h with a weight ratio between the catalyst and substrate, $R_{c/s}$ = 0.02.[25] Other metal oxide catalysts such as Co–Si-oxide[30] and $CuCr_2O_4$ [31] were also reported to catalyse the oxidative coupling of aniline. Higher temperatures (70 or 80 °C) were used in both cases to obtain higher than 70% conversion (Table S1†). Supported metal nanoparticles were also reported as catalysts for aniline oxidation with H_2O_2. For example, an Ag-WO_3 catalyst, in which the Ag nanoparticles were proposed to be the sites responsible for the activation of H_2O_2,[32] exhibited an aniline conversion of 87% with an azoxybenzene selectively of 91% at RT after 24 h employing a $R_{c/s}$ = 0.1. The non-noble metal catalyst Cu-CeO_2 was reported to display higher aniline conversion and azoxybenzene selectivity compared to the Ag-WO_3 catalyst after 6 h with the same $R_{c/s}$, although using 50 °C as the reaction temperature.[33] Control tests showed that the Cu nanoparticles acted as catalytic sites while CeO_2 performed as a support. The above-mentioned catalytic systems achieve good performance but still have some limitations, which can be related to the synthesis of the catalysts (*e.g.* synthesis requiring expensive templates[26–33] or dangerous chemicals such as hexafluorosilicic acid[24]) and/or to the employed conditions in which the oxidation of aniline is carried out (*e.g.* relatively high reaction temperatures,[23,24,26,28,29,31,33] problematic or hazardous solvents[26,27,29–33] and/or high loading of the catalyst, *e.g.* $R_{c/s}$ > 0.1, see Table S1†).[23,27,29,31–33] On this backdrop, we report the novel synthesis of amorphous Nb_2O_5 nanoparticles in supercritical CO_2 medium and their application as a heterogeneous catalyst with superior performance for the oxidative coupling of aniline and its derivatives to produce (substituted) azoxybenzene. The catalyst allowed performing the reaction without external heating and with an extremely low catalyst loading ($R_{c/s}$ = 0.005) in a green solvent as ethanol,[34] displaying very high aniline conversion and azoxybenzene yield in a short reaction time. All these achievements represent an important green advance as they would allow carrying out the conversion of (potentially) bio-based aniline into a useful compound under extremely mild and green conditions.

A crucial factor in achieving a catalyst with enhanced activity was the development of a novel supercritical-CO_2-assisted precipitation method for the preparation of highly-dispersed Nb_2O_5 nanoparticles. CO_2 in the supercritical state ($scCO_2$) is an attractive reaction medium for preparing nanostructured oxide catalysts for the combination of its properties, which are intermediate between those of a liquid and a gas and can be easily tuned by changing the temperature and pressure. More specifically, $scCO_2$ has good dissolving ability that can be exploited to promote the contact between compounds with different physicochemical features (*e.g.* polar and apolar; gas and liquid). In addition, $scCO_2$ has high diffusivity and extremely low surface tension, which are very important for maximum preservation of the formed nanostructures when removing CO_2 from the system, which can be achieved simply by depressurisation.[35] It has been extensively reported that the formation of nanomaterials typically proceeds differently with the assistance of $scCO_2$.[36–38] Further advantages of the use of $scCO_2$ as a reaction medium include the low toxicity and low cost of carbon dioxide and the relatively mild conditions needed to achieve its supercritical point (T_c = 31.1 °C, p_c = 73.9 bar).

Experimental

Materials

Niobium chloride ($NbCl_5$), deionised water and ethanol were used for the preparation of the Nb_2O_5 materials. Commercially available Nb_2O_5 (Nb_2O_5-Comm), TiO_2-P25, and WO_3 (WO_3-Comm) were used as reference catalysts. For the catalytic tests, aniline, *ortho*-toluidine, *meta*-toluidine, *para*-toluidine, 2-ethylaniline, 3-ethylaniline, 4-ethylaniline, *para*-anisidine, and benzylamine were used as substrates, anisole was used as the internal standard for gas chromatography (GC) analysis, while aqueous H_2O_2 with different concentrations (10 wt%, 20 wt%, 30 wt% and 50 wt%) was employed as the oxidant. Ethanol, 1,4-dioxane, acetone, acetonitrile, 2-butanol, isopropanol and methanol were tested as reaction solvents. 2,2,6,6-Tetramethyl-1-piperidinyloxy (TEMPO) was used as a radical scavenger. The purity and supplier of all chemicals (except for 10 wt% and 20 wt% H_2O_2) used during this research are listed in Table S2.† All chemicals were used without any further purification. 10 wt% and 20 wt% H_2O_2 aqueous solutions were prepared by diluting 30 wt% H_2O_2 with deionised water.

Catalyst preparation

Nb_2O_5 was prepared using a $scCO_2$-assisted precipitation method, with a novel protocol developed by adapting the synthesis methods of other metal oxides in $scCO_2$ medium[36,38,39] and by applying it to a precipitation method inspired by those used in the literature to prepare Nb_2O_5.[40–42] The synthesis was carried out in a high-throughput $scCO_2$ reactor unit manufactured by Integrated Lab Solutions (ILS),[43] which consists of two modules: a batch reactor equipped with a borosilicate glass window to allow visualisation of the phase behaviour within the reactor, and a block with 10 batch reactors (Fig. S1†). The window reactor and the 10-reactor block can be used simultaneously with individual operation steps. Each reactor has a volume of 84 mL (30 mm internal diameter), can be stirred individually with a magnetic stirrer and is equipped with an automated closing valve that allows avoiding cross-contamination between the reactors. The reactors are heated with electric heating elements, pressurised with an ISCO pump and cooled with a water-circulation system. The high-throughput unit can operate at a temperature between 20 and 200 °C and at a CO_2 pressure between 1 and 200 bar. An automated depressurisation protocol and rupture disks prevent the risks of overpressure. In a typical synthesis of the Nb_2O_5-$scCO_2$ material, firstly a niobium precursor solution was prepared by dissolving 1.0 g $NbCl_5$ in 2 mL ethanol with magnetic stirring for 5 min. HCl was formed as a gaseous product, indicating the formation of niobium ethoxide species. Then, 10 mL deionised water and 3 mL ethanol were added slowly to the stirred solution over 5 min. Upon the addition of water, the liquid became gradually opaque. Next, the mixture was transferred into the $scCO_2$ reactor and stirred vigorously at 40 °C for 3 h. At this stage, the white reaction mixture behaved like a high-viscosity liquid. Then, the reactor was closed, heated up to 80 °C and pressurised with CO_2 to 140 bar while stirring (this process took around 1.5 h). The reaction mixture was allowed to react under $scCO_2$ conditions for 3 h. Then, the reactor was cooled down to 20 °C and CO_2 was removed by slow depressurisation with an average rate of 1.5 bar min^{-1}. The obtained white slurry was aged overnight and then washed thoroughly with deionised water over a Büchner filter until the pH of the filtered water became neutral. Next, the material was dried overnight at 100 °C and the resulting powder was thermally treated in a calcination oven at 200 °C for 4 h with a heating rate of 2 °C min^{-1}. The catalyst prepared by this method was named Nb_2O_5-$scCO_2$. The synthesis process is summarised in Fig. 1. Since no formation of a gel was observed during the reaction, but only a precipitate, the used synthesis method is referred to as a $scCO_2$-assisted precipitation method. The mass of the calcined powders was always above 90% of the theoretical yield of Nb_2O_5 (around 0.45 g for each batch reactor). The as-prepared Nb_2O_5 powder was also thermally treated at 800 °C for 4 h with a heating rate of 2 °C min^{-1} and used as a reference catalyst (Nb_2O_5-800°C). Another reference Nb_2O_5 catalyst (Nb_2O_5-Ref) was prepared in a round-bottom flask with a similar procedure but without the assistance of $scCO_2$. Briefly, 1.0 g $NbCl_5$ was dissolved in 2 mL ethanol by stirring for 5 min, after which 10 mL deionised water and 3 mL ethanol were added slowly in 5 min. Next, the solution was stirred at 40 °C for 3 h. Then, the mixture was heated up to 80 °C and stirred for another 3 h. After that, the obtained product was aged, dried, washed and thermally treated with the same procedure as that used for Nb_2O_5-$scCO_2$.

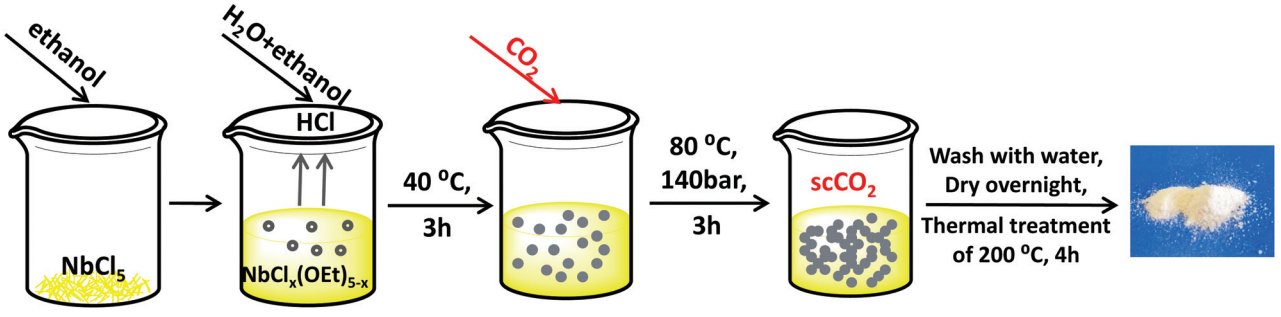

Fig. 1 Synthesis of Nb_2O_5-$scCO_2$ by a $scCO_2$-assisted precipitation method.

Characterisation

The Nb_2O_5 materials were characterised by a combination of techniques. N_2-Physisorption isotherms were recorded on a Micromeritics ASAP 2420 apparatus at −196 °C. The surface area was evaluated with the BET method. Before N_2 adsorption, the samples were degassed under reduced pressure at 200 °C for 5 h. X-ray diffraction patterns (XRD) were recorded on a Bruker D8 Phaser diffraction meter equipped with Cu Kα radiation (λ = 1.5406 Å). The XRD patterns were obtained in reflection geometry in the 2θ range between 10 and 80°. Fourier transform infrared spectroscopy (FTIR) measurements were performed with an IRTracer-100 spectrometer by averaging 64 scans with a spatial resolution of 4 cm^{-1}. The background spectrum was recorded by using an empty cell. Transmission electron microscopy (TEM) images were recorded using an electron microscope CM12 (Philips) operating at 120 keV. The samples were ground, then dispersed in ethanol by sonication and deposited on a holey-carbon-coated copper grid for TEM analysis. Scanning electron microscopy (SEM) analysis was carried out on a Philips XL30 ESEM microscope operating at 20 keV. The SEM samples were prepared by grinding the powder, dispersing it on carbon tape and spraying it with gold. Elemental analysis was carried out by using an inductively coupled plasma optical emission spectroscopy (ICP-OES) instrument. The samples were digested using HF before the analysis.

Catalytic experiments

The liquid-phase oxidation of aniline was carried out in a round-bottom flask equipped with a magnetic stirrer and water-cooled condenser. A soft rubber cap was placed on top of the condenser instead of a glass cap for safety reasons to prevent accidents in the event of blowing up of the cap caused by possible pressure build-up due to H_2O_2 decomposition (*vide infra*). In a typical experiment, 20 mmol aniline, 10 mmol anisole and the desired amount of H_2O_2 were added to 10 mL of solvent. Safety note: The reaction without any solvent under our optimum reaction conditions showed vigorous bubbling and using a solvent could avoid pressure build-up. Then, 10 mg catalyst was added and the reaction mixture was stirred for 45 min without external heating. After the reaction time was over, the stirring was stopped and *ca.* 30 mL of ethanol were added to ensure that the reaction mixture was in one phase. Then, the catalyst was separated by centrifugation at 4000 rpm for 3 min. The supernatant was analysed by means of an Agilent Technologies 7980B GC equipped with an Agilent DB-5#6 (5%-phenyl)-methylpolysiloxane column (15 m, 320 μm ID) and a flame ionisation detector. Safety note: Though the employed conditions did not pose any safety issue, care should be taken when using acetone and hydrogen peroxide together as they can form acetoneperoxide (explosive).

For the catalyst recycling tests, the rest of the supernatant was carefully removed by using a pipette. Then, *ca.* 45 mL ethanol was added to the centrifuge tube and the tube was shaken vigorously. After that, the tube was centrifuged at 4500 rpm for 20 min. Next, the supernatant was removed by using a pipette and *ca.* 45 mL fresh ethanol was added. This washing procedure was repeated 5 times. Then, the catalyst was dried at 100 °C overnight and regenerated by thermal treatment in a calcination oven at 200 °C for 4 h with a heating rate of 2 °C min^{-1} before reuse. For the leaching test, after 10 min of reaction the Nb_2O_5-$scCO_2$ catalyst was separated from the reaction mixture by centrifugation (4000 rpm, 3 min), followed by filtration with a filter connected to a syringe. A small aliquot of the filtrate was analysed by GC. The remaining filtrate was stirred for further 35 min at room temperature, after which the solution was analysed by GC.

The molar amounts of aniline and products (azoxybenzene, azobenzene, nitrobenzene and nitrosobenzene) were calculated using the following formula:

$$\mathrm{mmol}_x = \frac{\mathrm{Area}_x}{\mathrm{Area}_{\mathrm{IS}}} \times \mathrm{mmol}_{\mathrm{IS}} \times \frac{1}{\mathrm{Rf}_x}$$

where x is the compound whose molar amount is to be found and IS is the internal standard, *i.e.* anisole. Rf_x is the relative response factor of each compound (with respect to the IS) and was obtained by calibration of the commercial compound x with IS. The formulae used for the calculation of the aniline conversion, for the selectivity and yield of products and for the productivity (Prod), turn over number (TON) and turn over frequency (TOF) of the catalyst are as follows:

$$\mathrm{Conv.} = \frac{\mathrm{moles}_{\mathrm{aniline.\,init.}} - \mathrm{moles}_{\mathrm{aniline.\,end}}}{\mathrm{moles}_{\mathrm{aniline.\,init.}}} \times 100\%$$

$$\mathrm{Sel.}_x = \frac{n \times \mathrm{moles\ of\ product}\ x}{\mathrm{moles}_{\mathrm{aniline.\,init.}} - \mathrm{moles}_{\mathrm{aniline.\,end}}} \times 100\%$$

(n = 1 for nitrosobenzene and nitrobenzene, n = 2 for azobenzene and azoxybenzene)

$$\mathrm{Yield}_x = \mathrm{Conv.} \times \mathrm{Sel.}_x$$

$$\mathrm{Prod} = \frac{\mathrm{mass}_{\mathrm{azoxybenzene.end}}\,(\mathrm{g})}{\mathrm{mass}_{\mathrm{catalyst}}\,(\mathrm{g}) \times \mathrm{reaction\ time\ (h)}}$$

$$\mathrm{TON} = \frac{\mathrm{moles}_{\mathrm{azoxybenzene.end}}\,(\mathrm{mol})}{\mathrm{moles}_{\mathrm{catalyst}}\,(\mathrm{mol})}$$

$$\mathrm{TOF} = \frac{\mathrm{TON}}{\mathrm{reaction\ time\ (h)}}.$$

Results and discussion

In this work, we studied the aniline oxidative coupling to azoxybenzene using H_2O_2 as the oxidant under mild reaction conditions over a Nb_2O_5-$scCO_2$ catalyst. The catalyst was prepared by a novel $scCO_2$-assisted procedure; the ease, high yield and low cost of which are assets in the perspective of scale-up of the catalyst production. The choice of investigating Nb_2O_5 as the catalyst for the oxidation of aniline with H_2O_2 stems from the reported ability of this oxide to activate H_2O_2 for oxidation

reactions through the formation of active oxygen species, including peroxo, superoxo and hydroxyl radical species.[44,45] The exact form of active oxygen species depends on the active sites of the catalyst and the reaction conditions (*e.g.* pH, H_2O_2 concentration). Until now, Nb_2O_5 has been applied as a heterogeneous catalyst in many reactions employing H_2O_2 as the oxidant, such as the oxidation of organic sulfides,[44,45] glycerol, and alkenes.[46] Carreño *et al.* reported that Nb_2O_5 prepared by a microwave-assisted hydrothermal method catalysed the oxidation of aniline with H_2O_2 at 25 °C with phenylhydroxylamine and nitrosobenzene as the main products.[14] To the best of our knowledge, the application of Nb_2O_5 in aniline oxidation with azoxybenzene as the product has not been reported yet. On the other hand, two heterogeneous catalysts containing Nb in their formulation have been recently reported in aniline oxidation with H_2O_2 to produce azoxybenzene. NbOOH supported on FeOOH was reported to reach full aniline conversion with 70% azoxybenzene selectivity after 25 h at RT, though this required a relatively high $R_{c/s}$ of 0.1 (see Table S1†).[47] A Nb–Zn–Al-oxide catalyst (~4 wt% Nb loading, $R_{c/s}$ = 0.1) was reported to reach 92% azoxybenzene yield in the presence of UV irradiation for 48 h, whereas the yield dropped to 0% without irradiation.[48]

The initial test with Nb_2O_5-$scCO_2$ as a heterogeneous catalyst for the oxidation of aniline to azoxybenzene with aqueous H_2O_2 as the oxidant was carried out without external heating and with a low catalyst loading ($R_{c/s}$ = 0.005) compared to the values generally employed in the literature (Table S1†). Under these challenging conditions, an excellent aniline conversion of 86% was achieved in 45 min (stoichiometric maximum 93% with the employed H_2O_2 ratio of 1.4), with an azoxybenzene selectivity of 92% (Table 1, entry 1). The productivity of the Nb_2O_5-$scCO_2$ catalyst is remarkably high (209 grams of azoxybenzene generated per gram of catalyst in 1 h), which is more than double compared to that of the previous optimum and around two orders of magnitude larger than most of the catalysts reported in the literature (Table S1†). Additionally, the TON and TOF values for the Nb_2O_5-$scCO_2$ catalyst after 45 min of reaction were calculated to be 129 and 172 h^{-1}, respectively, based on the Nb content (57 wt%) of Nb_2O_5-$scCO_2$ obtained by ICP-OES analysis. The catalytic performance of Nb_2O_5-$scCO_2$ was directly compared under the same reaction conditions to that of selected commercial catalysts (Nb_2O_5-Comm, TiO_2-P25, and WO_3-Comm), which were chosen since they have been extensively reported to be able to activate H_2O_2 towards oxidation reactions (Table 1, entries 2–4).[23,46,49] Only minor amounts (<5%) of aniline could be converted and the only product was nitrosobenzene over these reference catalysts, and even TiO_2-P25, which had been reported to catalyse this reaction at 60 °C,[24] gave only slightly higher conversion at room temperature compared to a blank reaction (entries 3 and 5 in Table 1). A control experiment with Nb_2O_5-$scCO_2$ as the catalyst but without the use of H_2O_2 gave almost no conversion of aniline (Table 1, entry 6), thus confirming the need of H_2O_2 as the oxidant and excluding a significant contribution of oxygen from air as the oxidant.

A leaching test was performed to evaluate the heterogeneous nature of the Nb_2O_5-$scCO_2$ catalyst. After 10 min of reaction, the Nb_2O_5-$scCO_2$ catalyst was separated from the reaction mixture. At this stage, the aniline conversion was 4%. The filtrate was stirred for further 35 min at room temperature. No further increase in aniline conversion was observed (Fig. S2†), which indicates that no or negligible leaching of active species occurred, thus demonstrating that the Nb_2O_5-$scCO_2$ catalyst is truly heterogeneous. Importantly, based on the results of the catalytic test with Nb_2O_5-$scCO_2$, the H_2O_2 utilisation efficiency was calculated to be 95%, which indicates that the Nb_2O_5-$scCO_2$ catalyst was highly selective in activating H_2O_2 towards the conversion of aniline against the competitive decomposition into H_2O and O_2. Further insight into the catalytic reaction was provided by a kinetic study during which the temperature of the reaction mixture was monitored (Fig. S2†). The exothermic nature of the reaction led to a notable increase of the temperature of the reaction mixture after 25 min reaction time, reaching 77 °C at around 37 min reaction time, which corresponds to the time at which the maximum in aniline conversion was reached. At that moment, we also observed a bubbling phenomenon which was most probably related to the decomposition of residual H_2O_2 by the catalyst. These data suggest that the heat from the exothermic reaction promoted

Table 1 Activity of Nb_2O_5-$scCO_2$ and reference heterogeneous catalysts in the conversion of aniline to azoxybenzene

			Yield (%)				Selectivity (%)			
Entry	Catalyst	Conversion[a] (%)	Azoxy.	Nitroso.	Nitro.	Azo.	Azoxy.	Nitroso.	Nitro.	Azo.
1	Nb_2O_5-$scCO_2$	86	79	4	2	1	92	5	2	1
2	Nb_2O_5-Comm	4	0	4	0	0	0	>99	0	0
3	TiO_2-P25	5	0	5	0	0	0	>99	0	0
4	WO_3-Comm	3	0	3	0	0	0	>99	0	0
5	Blank[b]	2	0	2	0	0	0	>99	0	0
6	Nb_2O_5-$scCO_2$ [c]	<1	0	<1	0	0	0	>99	0	0
7	Nb_2O_5-$scCO_2$ [d]	5	0	5	0	0	0	>99	0	0
8	Nb_2O_5-800°C	4	0	4	0	0	0	>99	0	0

Reaction conditions: 20 mmol aniline, 28 mmol of H_2O_2 (as 30 wt% aqueous solution), 10 mmol anisole, 10 mL ethanol, 10 mg of the selected catalyst ($R_{c/s}$ = 0.005), no applied heating, 45 min. [a] Under the employed reaction conditions (aniline : H_2O_2 = 1 : 1.4), the theoretical maximum conversion is 93%. [b] Without a catalyst. [c] Without H_2O_2. [d] In the presence of TEMPO (1 mol% to H_2O_2) as a radical scavenger.

the decomposition of H_2O_2 and that, in turn, the complete consumption of H_2O_2 caused by the decomposition reaction prevented further conversion of aniline. The increase of the temperature of the solution as the exothermic reaction proceeded, also explains the observed gradual increase in the reaction rate (compare the conversion rate between 15 and 30 min with that between 30 and 40 min in Fig. S2b†).

Different mechanisms have been proposed for the activation of hydrogen peroxide by Nb_2O_5 catalysts, involving the formation of active oxygen species, among which metal (hydroxy)peroxo species and hydroxyl radicals are the most common.[46,50] In order to gain more insight into how Nb_2O_5-$scCO_2$ activates H_2O_2 towards the oxidation of aniline, a control experiment was conducted under the optimum reaction conditions but with the addition of TEMPO (1 mol% relative to H_2O_2), which has been widely reported to act as a hydroxyl radical scavenger.[51,52] A drastic decrease in the conversion of aniline to 5% was observed (Table 1, entry 7). In light of the above experimental findings, the aniline oxidative coupling with H_2O_2 is proposed to follow a free-radical mechanism. The catalytic cycle most likely starts with the formation of niobium hydroperoxo (Nb-OOH) species through the reaction between surface niobium-hydroxyls (Nb-OH) and H_2O_2.[46,50] Then, the interaction between Nb-OOH and H_2O_2 can generate highly reactive hydroxyl radicals ($^{\bullet}OH$) and hydroperoxo radicals ($^{\bullet}OOH$) and/or niobium peroxo radicals ($NbO_2^{\bullet}$) (Scheme S1†). This mechanism is supported by previous spectrosocopic studies, which identified the formation of all these three radical species when metal-hydroperoxo species interact with H_2O_2.[46,53] The formed radicals lead to the oxidation of aniline to form phenylhydroxylamine and nitrosobenzene (Scheme 1 and S1†), which in turn can react with each other through a condensation reaction yielding azoxybenzene and water as the final products (Scheme 1). The final condensation step can be catalysed by the Brønsted acid sites provided by the –OH groups on the surface of the Nb_2O_5-$scCO_2$ catalyst, which have been reported to be able to catalyse other dehydration reactions.[40–42]

The results obtained with Nb_2O_5-$scCO_2$ using a $R_{c/s}$ = 0.005 suggested that our catalyst might perform well at an even lower catalyst loading. Therefore, we carried out a kinetic test with a $R_{c/s}$ = 0.002 while maintaining the other reaction conditions. The aniline conversion reached 85% with an azoxybenzene selectivity of 88% after 60 min, which remained constant at longer reaction times (Fig. 2a). The side products were 5% of nitrosobenzene, 5% of nitrobenzene and 2% of azobenzene. The TOF value with this lower catalyst loading (calculated after 60 min of reaction) was even more notable, reaching 305 h^{-1}. This result proves that the Nb_2O_5-$scCO_2$ catalyst is able to reach very high aniline conversion also with this extremely low catalyst loading. These conditions were also employed for a comparison between Nb_2O_5-$scCO_2$ and a catalyst prepared with the same procedure but without the involvement of $scCO_2$ (Nb_2O_5-Ref). The comparison was based on a kinetic test in which we monitored the conversion of aniline and the selectivity of products as a function of reaction time

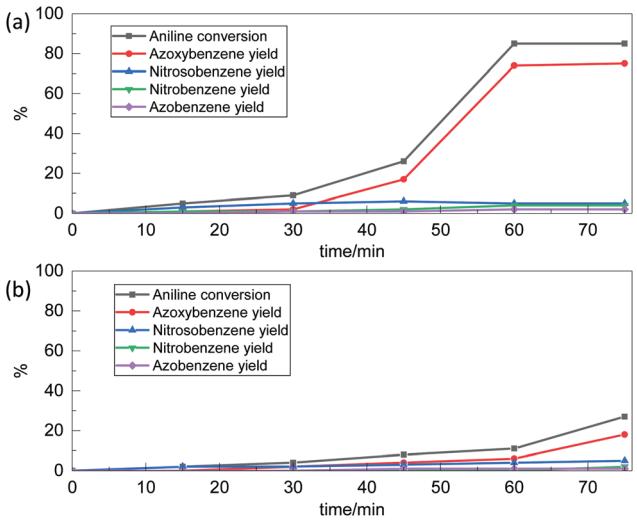

Fig. 2 Conversion of aniline with (a) Nb_2O_5-$scCO_2$ and (b) Nb_2O_5-Ref catalyst as a function of time. Reaction conditions: 50 mmol aniline, 70 mmol 30 wt% H_2O_2, 25 mmol anisole, 25 mL ethanol, 10 mg selected catalyst, no applied heating, 75 min.

by GC analysis (Fig. 2) and visually (Fig. S3†). These results indicate that Nb_2O_5-$scCO_2$ was able to catalyse the reaction much faster than Nb_2O_5-Ref. The conversion of aniline over Nb_2O_5-$scCO_2$ reached the maximum (85%) within 60 min, whereas only 11% conversion of aniline with 55% selectivity of azoxybenzene was achieved over Nb_2O_5-Ref at the same reaction time. This difference in activity was also reflected by the significantly lower TOF for the Nb_2O_5-Ref catalyst (24 h^{-1}, calculated after 60 min of reaction based on the 59 wt% Nb content determined by ICP-OES) compared to that for Nb_2O_5-$scCO_2$.

With the purpose of correlating the remarkable catalytic performance of Nb_2O_5-$scCO_2$ to its physicochemical properties, we performed a characterisation study by means of N_2-physisorption, XRD, FTIR and TEM. The textural properties of selected catalysts were investigated by N_2-physisorption. The adsorption–desorption isotherms of Nb_2O_5-$scCO_2$ and Nb_2O_5-Ref belong to type IV and have hysteresis loops at high p/p^0 values (Fig. 3), which are attributed to the presence of interparticle void spaces at the mesopore scale. Nb_2O_5-$scCO_2$ exhibits a slightly higher specific surface area compared to Nb_2O_5-Ref (340 $m^2\ g^{-1}$ *vs.* 305 $m^2\ g^{-1}$), and both of them are significantly higher than those of the commercial materials used as reference catalysts (Nb_2O_5-Comm: 5 $m^2\ g^{-1}$; TiO_2-P25: 65 $m^2\ g^{-1}$; WO_3-Comm: 3 $m^2\ g^{-1}$). The surface areas of Nb_2O_5-$scCO_2$ and Nb_2O_5-Ref are also higher than those of Nb_2O_5 materials synthesised by different routes but with similar (200 °C)[54] or even lower (60 or 80 °C)[40,42] temperature of the thermal treatment, which range between 142 and 184 $m^2\ g^{-1}$. The high surface area of Nb_2O_5-$scCO_2$ can contribute to the explanation of its catalytic activity as it implies a higher number of exposed active sites that are easily accessible to the reactants per gram of material, particularly compared to the commercial catalysts

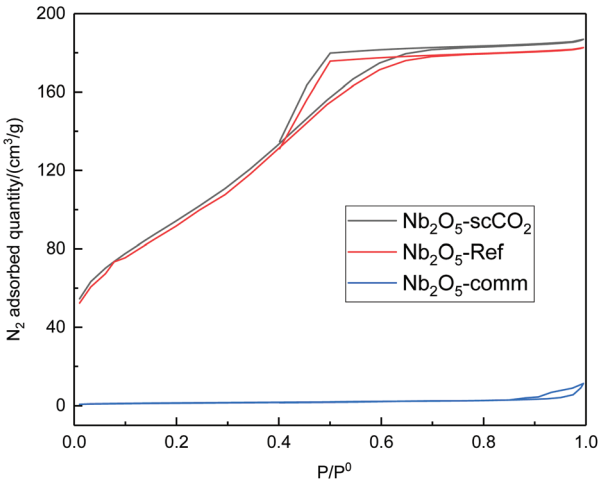

Fig. 3 N_2 adsorption–desorption isotherms of Nb_2O_5-$scCO_2$, Nb_2O_5-Ref and Nb_2O_5-Comm.

displaying very low surface areas (Nb_2O_5-Comm, TiO_2-P25, and WO_3-Comm).

The crystallinity of the selected catalysts was examined by XRD measurements. The patterns of both Nb_2O_5-$scCO_2$ and Nb_2O_5-Ref display two characteristic broad peaks centred at around 28° and 53°, corresponding to the amorphous Nb_2O_5 structure that consists of NbO_4 tetrahedra and NbO_6 octahedra (Fig. 4).[14,55] The amorphous nature of these two materials contrasts with the crystalline structure of Nb_2O_5-Comm (Fig. 4), with the pattern corresponding to the orthorhombic phase mainly consisting of NbO_6 octahedra (JCPDS No. 00-028-0317).[14,56] Crystalline Nb_2O_5 is typically obtained through a thermal treatment of amorphous or low crystallinity materials, during which the –OH groups on the surface gradually condense. Therefore, the degree of crystallinity is generally reflected in the surface hydrophilicity, which can be estimated by FTIR analysis. The peaks centred at 1640 cm^{-1} in the FTIR spectra of Nb_2O_5-$scCO_2$ and Nb_2O_5-Ref are assigned to the –OH bending mode of physisorbed water.[40] The broad absorption peaks in the range of 2800–3600 cm^{-1} of these two spectra are assigned to –OH stretching vibrations of physisorbed water[40] and, in analogy to other amorphous metal oxides,[23,57] to surface hydroxyl groups. These signals indicate the hydrophilic nature of the surface of Nb_2O_5-$scCO_2$ and Nb_2O_5-Ref. On the other hand, these peaks are virtually absent in the spectrum of Nb_2O_5-Comm (Fig. 5), indicating the much lower hydrophilicity of this material. The FTIR spectra of Nb_2O_5-$scCO_2$ and Nb_2O_5-Ref are quite similar, referring to the amorphous Nb_2O_5 structure. The FTIR spectrum of Nb_2O_5-Comm showed a well-defined absorption peak at ~800 cm^{-1} and two shoulders at ~870 cm^{-1} and ~715 cm^{-1}, which are characteristic of the Nb_2O_5 orthorhombic crystalline structure,[56] in agreement with the XRD results, whereas such peaks are absent in the spectra of the amorphous Nb_2O_5-$scCO_2$ and Nb_2O_5-Ref (Fig. 5). Based on the XRD and FTIR analyses, the higher activity of Nb_2O_5-$scCO_2$ and Nb_2O_5-Ref compared to Nb_2O_5-Comm is ascribed to the larger surface area of the two amorphous materials and the presence of surface –OH groups on their surfaces. The combination of these two features implies a much higher density of surface niobium-hydroxyls, which are the proposed catalytic sites for the activation of H_2O_2 (see Scheme S1†). This hypothesis is further supported by the drastic decrease in the specific surface area (2 m^2 g^{-1}) and aniline conversion (4%, see Table 1, entry 8) observed by converting Nb_2O_5-$scCO_2$ into crystalline niobium oxide upon calcination at 800 °C (Fig. S4†).

The above characterisation still does not explain the observed difference in catalytic activity between Nb_2O_5-$scCO_2$ and Nb_2O_5-Ref (see Fig. 2). A clue in this sense is provided by the TEM analysis of the two materials. Nb_2O_5-$scCO_2$ consists of discrete nanoparticles with small size and narrow particle size distribution in the 4 to 9 nm range (Fig. 6a and Fig. S5†).

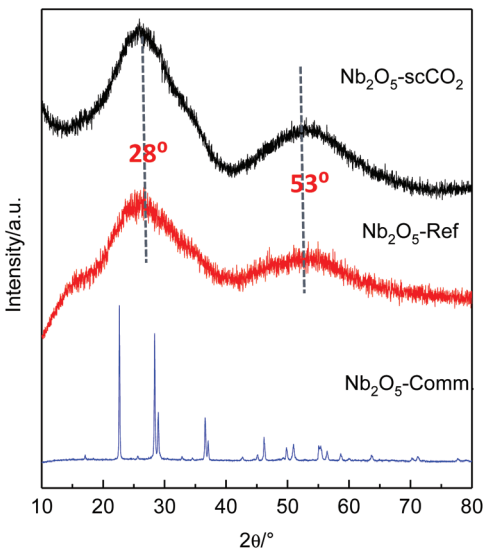

Fig. 4 XRD patterns of Nb_2O_5-$scCO_2$, Nb_2O_5-Ref and Nb_2O_5-Comm.

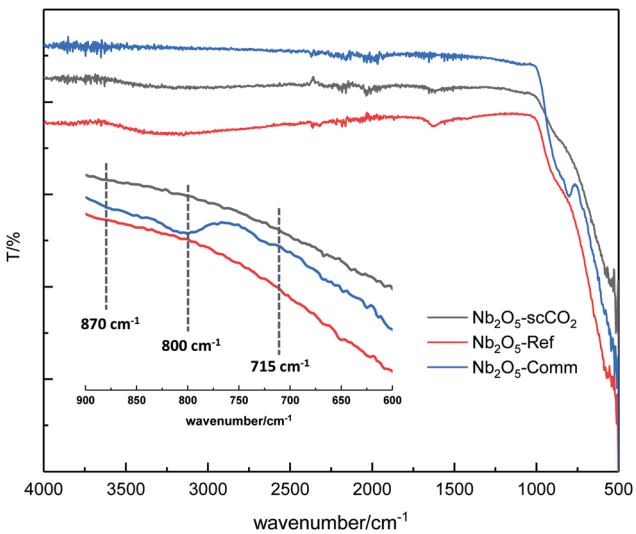

Fig. 5 FTIR spectra of Nb_2O_5-$scCO_2$, Nb_2O_5-Ref and Nb_2O_5-Comm. The small bands between 2000 and 2500 cm^{-1} present in all three spectra are due to the adsorption of CO_2 from air.

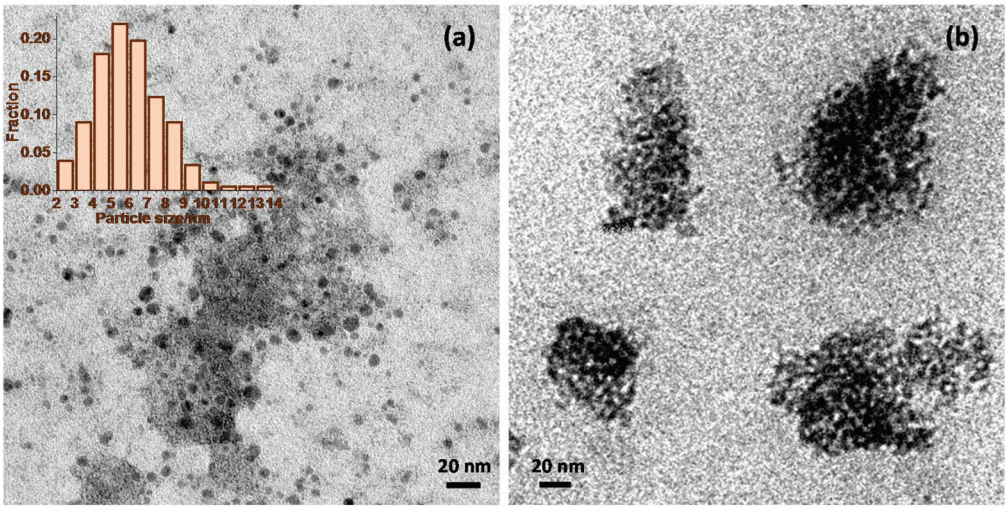

Fig. 6 TEM images of (a) Nb_2O_5-$scCO_2$ and (b) Nb_2O_5-Ref.

Some aggregated particles are also observed, though these might be caused simply by inadequate dispersion of the Nb_2O_5 nanoparticles in ethanol during the preparation of the TEM sample. On the other hand, the Nb_2O_5-Ref material prepared without $scCO_2$ mainly consists of aggregated larger particles with size between 50 to 100 nm (Fig. 6b). Such aggregation is probably caused by condensation reactions that are prevented if the synthesis is carried out in $scCO_2$ medium. The difference in morphology brought about by $scCO_2$ synthesis is likely to enable a better contact between the catalyst particles and the reactants in the liquid-phase oxidation of aniline, and would thus account for the superior catalytic activity of Nb_2O_5-$scCO_2$ compared to Nb_2O_5-Ref. The two materials were also characterised by SEM (Fig. S6†), though this analysis only indicates that for both catalysts the nanoparticles tend to aggregate into large secondary particles, which disaggregate once the materials are suspended in a liquid (as proven by the fact that such secondary particles are not observed by TEM).

Optimising the reaction conditions and catalyst reusability

Once the best catalyst for the oxidation of aniline to azoxybenzene was identified (Nb_2O_5-$scCO_2$), the reaction conditions were optimised with the aim of enhancing the aniline conversion and azoxybenzene selectivity. Firstly, the aniline-to-H_2O_2 ratio was optimised (Fig. 7). The theoretical stoichiometric ratio to achieve full conversion of aniline is 1 : 1.5 (see Scheme 1). When the reaction was performed with an understoichiometric amount of oxidant (1 : 1 ratio between aniline and H_2O_2), 63% of aniline conversion with an azoxybenzene selectivity of 98% was achieved over Nb_2O_5-$scCO_2$, which is very close to the maximum theoretical conversion under these conditions (67%). Upon increasing the relative amount of H_2O_2 so that full conversion is theoretically achievable, 92% of aniline conversion was obtained. Although this conversion with aniline-to-H_2O_2 ratio of 1 : 1.5 is higher than with 1 : 1.4, full conversion was not achieved and the azoxybenzene selectivity slightly decreased. This is attributed to the consumption of H_2O_2 caused by the formation of other side products and to H_2O_2 decomposition. For the 1 : 1.5 ratio between aniline and H_2O_2, the reaction was also performed by adding H_2O_2 dropwise for the first 15 minutes, with the aim of decreasing the chance of its decomposition and thus enhancing its utilisation. However, this did not prove beneficial and the aniline conversion and azoxybenzene selectivity obtained (data not shown) were the same as those obtained for the experiment in which all H_2O_2 was added initially. A further increase of the relative amount of H_2O_2 led to higher aniline conversion, eventually reaching full conversion for a 1 : 1.7 ratio between aniline and H_2O_2. However, under these conditions the selectivity towards azoxybenzene dropped to 84% with an increase in

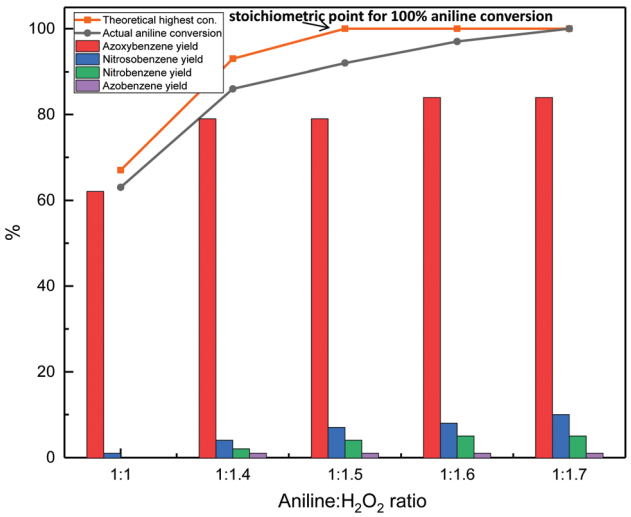

Fig. 7 Effect of aniline: H_2O_2 ratio on aniline conversion. Reaction conditions: 20 mmol aniline, 30 wt% H_2O_2 (20 to 34 mmol), 10 mmol anisole, 10 mL ethanol, 10 mg Nb_2O_5-$scCO_2$ catalyst, no applied heating, 45 min.

the formation of side products (*i.e.* nitrosobenzene, nitrobenzene and a trace amount of azobenzene). Nitrosobenzene was detected as the only side product when an aniline-to-H_2O_2 ratio of 1 : 1 was used. Nitrobenzene was also detected as a side product when an aniline-to-H_2O_2 ratio equal to 1 : 1.4 was used and with a higher relative amount of H_2O_2, with the yields of this compound increasing with the increasing of H_2O_2 amount as a consequence of over-oxidation of the reaction intermediates (Scheme 1). Since the yield of azoxybenzene achieved using a 1 : 1.4 ratio between aniline and H_2O_2 (79%) increased only in a minor way by increasing the relative amount of hydrogen peroxide, while this caused a gradual drop in azoxybenzene selectivity (92%), this ratio between the substrate and oxidant was employed in the following steps of this study.

Aqueous hydrogen peroxide is commercially available in different concentrations. The presence of water could be detrimental as it can compete with hydrogen peroxide for adsorption on the catalyst surface and could hinder the dehydration step from phenyhydroxylamine and nitrosobenzene to azoxybenzene. To test these hypotheses, the effect of using different concentrations of H_2O_2 was investigated (Fig. 8 and Fig. S7†). Although visual observation of the colour of the reaction mixture clearly indicated that the rate of azoxybenzene formation in the first 25 min of reaction was higher with the higher concentration of hydrogen peroxide (Fig. S7†), at the end of the catalytic test (45 min), the highest aniline conversion and azoxybenzene selectivity were obtained with 30 wt% H_2O_2 rather than with 50 wt% H_2O_2 (Fig. 8). In the literature, a higher rate of azoxybenzene formation was observed over a TiO_2 catalyst by employing hydrogen peroxide solutions with higher concentrations.[23] Such a relation between the H_2O_2 concentration and reaction rate can be ascribed to the lower dilution effect with a higher concentration of H_2O_2 solution, which would grant higher accessibility of aniline and H_2O_2 to the catalyst and lead to faster heat transfer with a consequent faster rise of the temperature of the reaction mixture and thus a higher reaction rate.[26,30,32,33] Additionally, the amount of water is the lowest with 50 wt% H_2O_2, thus probably facilitating the dehydration between phenylhydroxylamine and nitrosobenzene to form azoxybenzene. Although this trend is followed with our Nb_2O_5-$scCO_2$ catalyst in the first 25 min of reaction (Fig. S7†), it is valid over the whole catalytic test only for the H_2O_2 concentration up to 30 wt% (Fig. 8). The observed lower yield of azoxybenzene with 50 wt% H_2O_2 compared to 30 wt% H_2O_2 at the end of the catalytic test can be ascribed to the higher extent of H_2O_2 decomposition in the former case, as a consequence of a faster and larger temperature increase in the more concentrated reaction mixture. This hypothesis was supported by performing a test with the Nb_2O_5-$scCO_2$ catalyst using 1.7 times H_2O_2 (50 wt% aqueous solution) relative to aniline. Under these conditions, 94% aniline conversion with 87% azoxybenzene selectivity was obtained, compared to the full conversion of aniline achieved with 30 wt% H_2O_2 (Fig. 7), suggesting that a higher percentage of H_2O_2 was decomposed when 50 wt% H_2O_2 was used. In addition, according to the Global Harmonised System (GHS) for the classification and labelling of chemicals, 50 wt% H_2O_2 belongs to the GHS03 hazard category (oxidising liquid), which requires more rigid precautionary measures than 30 wt% H_2O_2. Therefore, the use of 30 wt% H_2O_2 is preferable not only because it gives higher utilisation efficiency of H_2O_2 with the Nb_2O_5-$scCO_2$ catalyst, but also in terms of safety concerns and, therefore, in the context of the green chemistry principles.

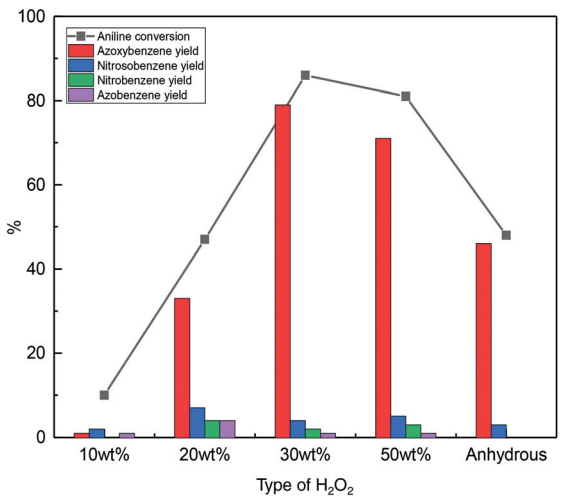

Fig. 8 Effect of H_2O_2 concentration on aniline conversion. Reaction conditions: 20 mmol aniline, 28 mmol of aqueous H_2O_2 (with the amount of H_2O being different in each test), 10 mmol anisole, 10 ml ethanol, 10 mg Nb_2O_5-$scCO_2$ catalyst, no applied heating, 45 min.

The solvent in which the reaction takes place was also optimised by screening a set of solvents with different polarities and aprotic/protic nature (Table 2). These solvents were selected because they form a single phase with aniline and the aqueous H_2O_2 solution, thus averting the mass transfer problem associated with the presence of different liquid phases. According to the CHEM21 guide for ranking the greenness of solvents,[34] the selected alcohols and acetone are recommended solvents, acetonitrile is recognised as a problematic solvent, whereas 1,4-dioxane is labelled as hazardous. The use of ethanol as a solvent led to the highest azoxybenzene yield (79%) and selectivity (92%), while isopropanol gave the highest aniline conversion (90%), which represents a slight improvement compared to that in ethanol (86%). Although there is no clear correlation between the catalytic activity and solvent polarity (Fig. S8†), in general the aniline conversion and azoxybenzene yield are higher in protic solvents compared to those in aprotic solvents. Such a positive effect of the protic solvents can be related to the radical mechanism over the Nb_2O_5-$scCO_2$ catalyst. It has been reported that the polarisation of hydroxyl radicals in protic solvents is stronger than that in aprotic solvents,[58] thus increasing the electrophilicity of the radical and promoting its reactivity. It should be noted that other solvent-related factors might play a role too, including the radical quenching ability of solvents,[59] their interaction with the catalyst surface and their solvating and stabilising effects on reactants, intermediates and products.[25,28,60,61]

Table 2 Effect of the solvent on the activity of the Nb_2O_5-$scCO_2$ catalyst in the oxidative coupling of aniline to azoxybenzene

Solvent	Aprotic (A) or protic (P)	Boiling point (°C)	Dipole moment (D)	Dielectric constant (at 25 °C)	Conversion[a] (%)	Yield (%)				Selectivity (%)			
						Azoxy	Nitroso	Nitro	Azo	Azoxy	Nitroso	Nitro	Azo
1,4-Dioxane	A	88	0.45	2.2	58	48	5	3	2	82	9	5	4
Acetone	A	56	2.85	20.7	54	45	4	3	3	83	7	5	5
Acetonitrile	A	82	3.92	37.5	78	52	17	6	3	66	22	8	4
2-Butanol	P	98	1.66	16.6	82	67	7	4	3	83	9	5	3
Isopropanol	P	83	1.66	17.9	90	77	8	4	1	86	9	4	1
Ethanol	P	78	1.69	24.3	86	79	4	2	1	92	5	2	1
Methanol	P	65	1.69	32.7	81	69	8	4	0	86	10	4	0

Reaction conditions: 20 mmol aniline, 28 mmol 30 wt% H_2O_2, 10 mmol anisole, 10 mL selected solvent, 10 mg Nb_2O_5-$scCO_2$ catalyst, no applied heating, 45 min. [a] Under the employed reaction conditions (aniline : H_2O_2 = 1 : 1.4), the theoretical maximum conversion is 93%.

Table 3 Activity of the Nb_2O_5-$scCO_2$ catalyst in the conversion of different substituted anilines

Anilines	Conversion (%)[a]	Selectivity (%)			
		Azoxy.	Nitroso.	Nitro.	Azo
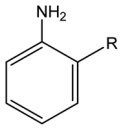	R: methyl = 78 R: ethyl = 81	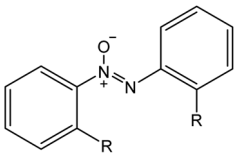 R: methyl = 47 R: ethyl =45	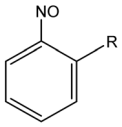 R: methyl = 53 R:ethyl =55		
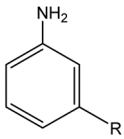	R: methyl = 82 R: ethyl = 84	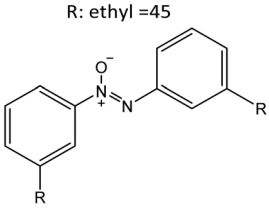 R: methyl = 72 R: ethyl =75	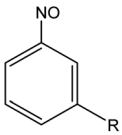 R: methyl = 21 R: ethyl =24	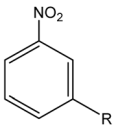 R: methyl = 6 R: ethyl =1	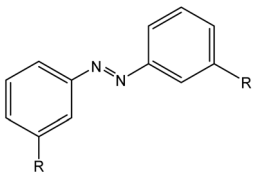 R: methyl < 1 R: ethyl < 1
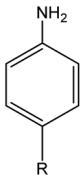	R: methyl = 81 R: ethyl = 81	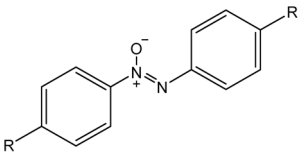 R: methyl = 80 R: ethyl =83	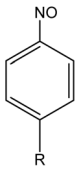 R: methyl = 20 R: ethyl =17		
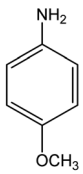 *para*-anisidine	53	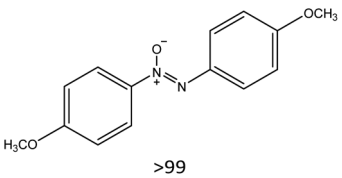 >99			
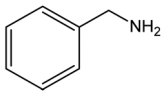 benzylamine	0				

Reaction conditions: 20 mmol substituted aniline, 28 mmol 30 wt% H_2O_2, 10 mmol anisole, 10 mL ethanol, 10 mg Nb_2O_5-$scCO_2$ catalyst, no applied heating, 45 min. [a] Under the employed reaction conditions (aniline : H_2O_2 = 1 : 1.4), the maximum theoretical conversion is 93%.

Finally, the recyclability of the Nb_2O_5-$scCO_2$ catalyst in consecutive runs under the optimum reaction conditions was tested (Fig. S9†), demonstrating that the catalyst fully retained its activity and selectivity in 4 consecutive runs (aniline conversion or azoxybenzene selectivity ±2%).

Substrate scope

Having established the best reaction conditions, we completed our study by investigating the scope of substrates that can be converted over Nb_2O_5-$scCO_2$ (Table 3). For this purpose, we selected substituted anilines with different types and positions of the substituting group. Some of these substituted anilines would afford azoxy products that can find application in pharmaceutical compounds (from alkyl-substituted anilines) and liquid crystals (from *para*-anisidine).[6,7] Nb_2O_5-$scCO_2$ efficiently catalysed the transformation of all investigated alkyl-substituted anilines with high conversion (≥78%), though the unsubstituted aniline affords the highest yield of the azoxy product in 45 min. Although the conversion of the alkyl substituted anilines is in the same range, the selectivity towards the azoxy product is strongly influenced by the presence and position of the alkyl group on the aromatic ring. Among the alkyl-substituted anilines, the highest selectivity towards the azoxy product was observed when the alkyl group was in the *para*-position, followed by the *meta* and *ortho* positions.[28,48] The main side product was the corresponding alkyl-nitrosobenzene, which becomes the major product with the *ortho*-substituted anilines. These results indicate that the alkyl substituents do not play a major role in the initial oxidation of the amino group with hydrogen peroxide, but have a relevant steric effect in the condensation step that leads to the formation of the azoxy product (Scheme 1). The reaction with *para*-anisidine achieved 53% conversion, which is lower compared to the conversion obtained with aniline and alkyl-substituted anilines. This is ascribed to the presence of the methoxy substituent, which is expected to increase the electron density of the $-NH_2$ group in *para*-anisidine as a consequence of the resonance effect of this substituent (dominating over its electron withdrawing inductive effect). The higher electron density on the amino group compared to that in aniline is detrimental to the radical-induced oxidation steps.[58] Furthermore, no conversion was observed using benzylamine as the substrate. The difficulty in converting benzylamine under the employed mild conditions is also related to electronic effects. Compared to aniline, the α carbon between the amino group and the aromatic ring in benzylamine disrupts the resonance effect, thus decreasing the electrophilicity of $-NH_2$ and thus negatively affecting its reactivity towards the hydroxyl radical species.

Conclusions

In this work, Nb_2O_5 nanoparticles with a high specific surface area (340 $m^2\ g^{-1}$) were prepared by a novel, supercritical-CO_2-assisted method and were applied as a heterogeneous catalyst for the oxidative coupling of aniline with H_2O_2 to produce azoxybenzene. The catalyst achieved excellent activity and selectivity towards azoxybenzene in a short time (45 min) under mild conditions (no applied heating) and with a catalyst loading that was much lower compared to those reported in the literature for this reaction. Full aniline conversion could be achieved by employing only a small excess of H_2O_2 compared to the stoichiometric amount, demonstrating a high efficiency of the catalyst in activating hydrogen peroxide towards the desired oxidation. A control test in the presence of a radical scavenger suggested that the reaction follows a free-radical pathway. The Nb_2O_5-$scCO_2$ catalyst does not suffer from leaching and can be reused in consecutive runs without losing activity. Notably, the catalyst is also versatile as it is active in the conversion of a variety of substituted anilines, though the selectivity towards the azoxy product is lower particularly for *ortho*-substituted substrates. The discrete nanoparticle morphology brought about by the utilisation of $scCO_2$ in the synthesis accounts for the much superior catalytic performance of Nb_2O_5-$scCO_2$ compared to the state-of-the-art catalysts for this reaction. The green aspects of this system include the use of an environmentally benign oxidant as H_2O_2, the extremely mild reaction conditions, the use of a green solvent as ethanol, the short reaction time, the extremely low catalyst loading and the high efficiency in the utilisation of H_2O_2. These features are also attractive from the perspective of an industrial application of this catalytic system. Additionally, the $scCO_2$-assisted method that led to the synthesis of this excellent Nb_2O_5 catalyst has the potential to be applied to the preparation of other metal–oxide heterogeneous catalysts.

Conflicts of interest

There are no conflicts to declare.

Acknowledgements

Yehan Tao acknowledges financial support from the China Scholarship Council (CSC) for her Ph.D. grant. The authors acknowledge Leon Rohrbach and Marcel de Vries for their analytical and technical support.

References

1 H. Takahashi, T. Ishioka, Y. Koiso, M. Sodeoka and Y. Hashimoto, *Biol. Pharm. Bull.*, 2000, **23**(11), 1387–1390.
2 A. B. Vix, P. Müller-Buschbaum, W. Stocker, M. Stamm and J. P. Rabe, *Langmuir*, 2000, **16**(26), 10456–10462.
3 D. Aronzon, E. P. Levy, P. J. Collings, A. Chanishvili, G. Chilaya and G. Petriashvili, *Liq. Cryst.*, 2007, **34**(6), 707–718.
4 E. Voutyritsa, A. Theodorou, M. G. Kokotou and C. G. Kokotos, *Green Chem.*, 2017, **19**(5), 1291–1298.
5 E. Buncel and B. T. Lawton, *Can. J. Chem.*, 1965, **43**(4), 862–875.

6 K. Selvam, S. Balachandran, R. Velmurugan and M. Swaminathan, *Appl. Catal., A*, 2012, **413**, 213–222.
7 I. W. Stewart, *Book: The static and dynamic continuum theory of liquid crystals*, 2004, p. 17.
8 H. Li, X. Xie and L. Wang, *Chem. Commun.*, 2014, **50**(32), 4218–4221.
9 L. Liu, P. Concepción and A. Corma, *J. Catal.*, 2019, **369**, 312–323.
10 Q. Xiao, Z. Liu, F. Wang, S. Sarina and H. Zhu, *Appl. Catal., B*, 2017, **209**, 69–79.
11 Z. Liu, Y. Huang, Q. Xiao and H. Zhu, *Green Chem.*, 2016, **18**(3), 817–825.
12 B. Zhou, J. Song, T. Wu, H. Liu, C. Xie, G. Yang and B. Han, *Green Chem.*, 2016, **18**(13), 3852–3857.
13 https://www.covestro.com/en/sustainability/lighthouse-projects/bio-aniline.
14 W. M. Ventura, D. C. Batalha, H. V. Fajardo, J. G. Taylor, N. H. Marins, B. S. Noremberg, T. Tański and N. L. Carreño, *Catal. Commun.*, 2017, **99**, 135–140.
15 Y. Shiraishi, H. Sakamoto, K. Fujiwara, S. Ichikawa and T. Hirai, *ACS Catal.*, 2014, **4**(8), 2418–2425.
16 A. Grirrane, A. Corma and H. García, *Science*, 2008, **322**(5908), 1661–1664.
17 F. Yang, Z. Wang, X. Zhang, L. Jiang, Y. Li and L. Wang, *ChemCatChem*, 2015, **7**(21), 3450–3453.
18 K. Ju and R. E. Parales, *Microbiol. Mol. Biol. Rev.*, 2010, **74**(2), 250–272.
19 M. I. Qadir, J. D. Scholten and J. Dupont, *Catal. Sci. Technol.*, 2015, **5**(3), 1459–1462.
20 W. D. Emmons, *J. Am. Chem. Soc.*, 1957, **79**(20), 5528–5530.
21 R. W. Murray, R. Jeyaraman and L. Mohan, *Tetrahedron Lett.*, 1986, **27**(21), 2335–2336.
22 A. Mckillop and J. A. Tarbin, *Tetrahedron*, 1987, **43**(8), 1753–1758.
23 H. Tumma, N. Nagaraju and K. V. Reddy, *Appl. Catal., A*, 2009, **353**(1), 54–60.
24 L. Yang, G. Shi, X. Ke, R. Shen and L. Zhang, *CrystEngComm*, 2014, **16**(9), 1620–1624.
25 N. Jagtap and V. Ramaswamy, *Appl. Clay Sci.*, 2006, **33**(2), 89–98.
26 S. Gontier and A. Tuel, *Appl. Catal., A*, 1994, **118**(2), 173–186.
27 H. Sonawane, A. V. Pol, P. P. Moghe, S. S. Biswas and A. Sudalai, *J. Chem. Soc., Chem. Commun.*, 1994, **10**, 1215–1216.
28 D. R. Das and A. K. Talukdar, *ChemistrySelect*, 2017, **2**(28), 8983–8989.
29 S. Gontier and A. Tuel, *J. Catal.*, 1995, **157**(1), 124–132.
30 C.-F. Chang and S.-T. Liu, *J. Mol. Catal. A: Chem.*, 2009, **299**(1–2), 121–126.
31 S. S. Acharyya, S. Ghosh and R. Bal, *ACS Sustainable Chem. Eng.*, 2014, **2**(4), 584–589.
32 S. Ghosh, S. S. Acharyya, T. Sasaki and R. Bal, *Green Chem.*, 2015, **17**(3), 1867–1876.
33 A. Shukla, R. K. Singha, L. S. Konathala, T. Sasaki and R. Bal, *RSC Adv.*, 2016, **6**(27), 22812–22820.
34 D. Prat, A. Wells, J. Hayler, H. Sneddon, C. R. McElroy, S. Abou-Shehada and P. J. Dunn, *Green Chem.*, 2015, **18**(1), 288–296.
35 Y. Tao and P. P. Pescarmona, *Catalysts*, 2018, **8**(5), 212.
36 M. B. Chowdhury, R. Sui, R. A. Lucky and P. A. Charpentier, *Langmuir*, 2009, **26**(4), 2707–2713.
37 J. Yoo, Y. Bang, S. J. Han, S. Park, J. H. Song and I. K. Song, *J. Mol. Catal. A: Chem.*, 2015, **410**, 74–80.
38 J. Jammaer, C. Aprile, S. W. Verbruggen, S. Lenaerts, P. P. Pescarmona and J. A. Martens, *ChemSusChem*, 2011, **4**(10), 1457–1463.
39 N. Farhangi, R. R. Chowdhury, Y. Medina-Gonzalez, M. B. Ray and P. A. Charpentier, *Appl. Catal., B*, 2011, **110**, 25–32.
40 K. Nakajima, Y. Baba, R. Noma, M. Kitano, J. N. Kondo, S. Hayashi and M. Hara, *J. Am. Chem. Soc.*, 2011, **133**(12), 4224–4227.
41 M. T. Reche, A. Osatiashtiani, L. J. Durndell, M. A. Isaacs, Â. Silva, A. F. Lee and K. Wilson, *Catal. Sci. Technol.*, 2016, **6**(19), 7334–7341.
42 C. Yue, G. Li, E. A. Pidko, J. J. Wiesfeld, M. Rigutto and E. J. Hensen, *ChemSusChem*, 2016, **9**(17), 2421–2429.
43 A. J. Kamphuis, F. Milocco, L. Koiter, P. P. Pescarmona and E. Otten, *ChemSusChem*, 2019, **12**, 1–8.
44 J. V. Coelho, M. Guedes, G. Mayrink, P. P. Souza, M. C. Pereira and L. C. Oliveira, *New J. Chem.*, 2015, **39**(7), 5316–5321.
45 A. Bozzi, R. Lavall, T. Souza, M. Pereira, P. De Souza, H. De Abreu, A. De Oliveira, P. Ortega, R. Paniago and L. C. A. Oliveira, *Dalton Trans.*, 2015, **44**(46), 19956–19965.
46 M. Ziolek, I. Sobczak, P. Decyk, K. Sobańska, P. Pietrzyk and Z. Sojka, *Appl. Catal., B*, 2015, **164**, 288–296.
47 A. L. Lima, D. C. Batalha, H. V. Fajardo, J. L. Rodrigues, M. C. Pereira and A. C. Silva, *Catal. Today*, 2018, DOI: 10.1016/j.cattod.2018.10.035.
48 G. S. de Carvalho, L. H. Chagas, C. G. Fonseca, P. P. De Castro, A. C. Sant, A. A. Leitão and G. W. Amarante, *New J. Chem.*, 2019, **43**, 5863.
49 C. Hammond, J. Straus, M. Righettoni, S. E. Pratsinis and I. Hermans, *ACS Catal.*, 2013, **3**(3), 321–327.
50 I. D. Ivanchikova, I. Y. Skobelev, N. V. Maksimchuk, E. A. Paukshtis, M. V. Shashkov and O. A. Kholdeeva, *J. Catal.*, 2017, **356**, 85–99.
51 S. S. Acharyya, S. Ghosh and R. Bal, *Chem. Commun.*, 2014, **50**(87), 13311–13314.
52 S. S. Acharyya, S. Ghosh and R. Bal, *Chem. Commun.*, 2015, **51**(27), 5998–6001.
53 M. Ziolek, P. Decyk, I. Sobczak, M. Trejda, J. Florek, H. G. W. Klimas and A. Wojtaszek, *Appl. Catal., A*, 2011, **391**(1–2), 194–204.
54 H. T. Kreissl, K. Nakagawa, Y.-K. Peng, Y. Koito, J. Zheng and S. C. E. Tsang, *J. Catal.*, 2016, **338**, 329–339.
55 M. N. Catrinck, E. S. Ribeiro, R. S. Monteiro, R. M. Ribas, M. H. Barbosa and R. F. Teófilo, *Fuel*, 2017, **210**, 67–74.
56 M. Graça, A. Meireles, C. Nico and M. Valente, *J. Alloys Compd.*, 2013, **553**, 177–182.

57 A. J. Bonon, Y. N. Kozlov, J. O. Bahú, R. Maciel Filho, D. Mandelli and G. B. Shul'pin, *J. Catal.*, 2014, **319**, 71–86.
58 S. Mitroka, S. Zimmeck, D. Troya and J. M. Tanko, *J. Am. Chem. Soc.*, 2010, **132**(9), 2907–2913.
59 A. Brizzolari, G. M. Campisi, E. Santaniello, N. Razzaghi-Asl, L. Saso and M. C. Foti, *Biophys. Chem.*, 2017, **220**, 1–6.
60 A. G. da Silva, D. C. Batalha, T. S. Rodrigues, E. G. Candido, S. C. Luz, I. C. de Freitas, F. C. Fonseca, D. C. de Oliveira, J. G. Taylor, S. I. C. de Torresi, P. H. C. Camargo and H. V. Fajardo, *Catal. Sci. Technol.*, 2018, **8**(7), 1828–1839.
61 S. B. Waghmode, S. M. Sabne and S. Sivasanker, *Green Chem.*, 2001, **3**(6), 285–288.